



Contents lists available at ScienceDirect

Biochemical and Biophysical Research Communications

journal homepage: www.elsevier.com/locate/ybbrc



Picropodophyllin inhibits tumor growth of human nasopharyngeal carcinoma in a mouse model



Shu-Cheng Yin^{a,b}, Wei Guo^b, Ze-Zhang Tao^{a,*}

^a Department of Otolaryngology – Head and Neck Surgery, Renmin Hospital of Wuhan University, Wuhan 430060, PR China

^b Department of Otolaryngology – Head and Neck Surgery, Zhongnan Hospital of Wuhan University, Wuhan 430071, PR China

ARTICLE INFO

Article history:

Received 11 August 2013

Available online 22 August 2013

Keywords:

Nasopharyngeal carcinoma
Insulin-like growth factor-1 receptor
Picropodophyllin
Akt
Nude mouse

ABSTRACT

Insulin-like growth factor-1 receptor (IGF-1R) is a cell membrane receptor with tyrosine kinase activity and plays important roles in cell transformation, tumor growth, tumor invasion, and metastasis. Picropodophyllin (PPP) is a selective IGF-1R inhibitor and shows promising antitumor effects for several human cancers. However, its antitumor effects in nasopharyngeal carcinoma (NPC) remain unclear. The purpose of this study is to investigate the antitumor activity of PPP in NPC using *in vitro* cell culture and *in vivo* animal model. We found that PPP dose-dependently decreased the IGF-induced phosphorylation and activity of IGF-1R and consequently reduced the phosphorylation of Akt, one downstream target of IGF-1R. In addition, PPP inhibited NPC cell proliferation *in vitro*. The half maximal inhibitory concentration (IC₅₀) of PPP for NPC cell line CNE-2 was $\leq 1 \mu\text{M}$ at 24 h after treatment and $\leq 0.5 \mu\text{M}$ at 48 h after treatment, respectively. Moreover, administration of PPP by intraperitoneal injection significantly suppressed the tumor growth of xenografted NPC in nude mice. Taken together, these results suggest targeting IGF-1R by PPP may represent a new strategy for treatment of NPCs with positive IGF-1R expression.

© 2013 Elsevier Inc. All rights reserved.

1. Introduction

Nasopharyngeal carcinoma (NPC) is a relative uncommon disease in Europe and North America where its incidence is less than 1 per 100,000 [1,2]; however, NPC is a very common disease in southeast Asia, particularly in southern China with a rather high incidence of 25 per 100,000 [2,3]. Although the exact mechanisms are not very clear yet, it is believed that multiple factors including genetic, ethnic, and dietary factors as well as Epstein–Barr virus infection contribute to the development of NPC [2–4]. Due to the advances of technology in diagnosis and in radio-/chemo-therapy, overall survival of NPC patients can sometimes achieve up to 70–75% at 5 years [4]; however, there are still about 25–30% patients failed to these treatments, and patients with local recurrence and/or distant metastasis usually have poor prognosis [5]. Therefore, new therapeutic strategy is necessary for those patients failed to response to the current treatments.

Insulin-like growth factor-1 receptor (IGF-1R) is a member of receptor tyrosine kinase family proteins, which are usually deregulated in human cancers [6–8]. Actually, high expression or overexpression of IGF-1R has been associated with aggressive phenotype, tumor progression, and poor outcome in several human

cancers including ovary cancer, breast cancer, prostate cancer, colorectal cancer, melanoma, sarcoma, leukemia, and myeloma etc., and IGF-1R is therefore a potential therapeutic target for these cancers [9]. Picropodophyllin (PPP), a new selective inhibitor of IGF-1R, has been received more attention lately because of its high specificity and little toxicity [10]. PPP strongly inhibits malignant cell growth both *in vitro* and in animal models for uveal melanoma [11], glioblastoma [12], breast cancer [13], ovarian cancer [14], and multiple myeloma [15]. However, there is no study currently available about targeting IGF-1R by PPP in nasopharyngeal cancers.

We previously demonstrated that IGF-1R is highly expressed in NPC cells, and its expression level significantly associates with tumor progression [16]. This raises an interesting possibility that targeting IGF-1R by PPP may be a new therapeutic strategy for advanced NPC. Here we investigated the antitumor effects of PPP on NPC by targeting IGF-1R in both *in vitro* and *in vivo* models.

2. Materials and methods

2.1. Reagents

PPP was kindly provided by Professor Olle Larrson (Department of Oncology-Pathology, Karolinska Institutet, Stockholm, Sweden) and dissolved in DMSO before addition to the cells or

* Corresponding author.

E-mail address: zezhangtao@gmail.com (Z.-Z. Tao).

intraperitoneal injection of mice. Iove's Modified Dulbecco's Medium (IMDM) was bought from GIBCO; Antibodies of phosphorylated IGF-1R (pY99) monoclonal antibody, alpha-subunit polyclonal antibody (N20), beta-subunit polyclonal antibody (C20, H-60), phosphorylated Akt (pS473) antibody, total Akt antibody (H-136), phosphorylated Erk (pT202/Y204) antibody, and total Erk (E-16) antibody were all from Santa Cruz; Vincristine was from Sigma.

Sixteen BALB/c nude mice (4–5 weeks old) were from the animal center of the Hubei Center of Disease Control and Prevention and kept in SPF animal room at Wuhan University. Human NPC cell line CNE-2 derived from human poorly differentiated nasopharyngeal carcinoma [17] was provided by the Tissue and Cell Collection Center of Wuhan University. CNE-2 cells were maintained in IMDM medium containing 10% FBS and 100 U/ml penicillin with 100 µg/ml streptomycin at 37 °C in 5% CO₂.

2.2. Immunoprecipitation and Western blot assay

CNE-2 cells cultured in 6-well plate were serum starved for 20 h and then treated with different concentrations of PPP for 1 h followed by IGF-1 stimulation (50 ng/ml) for 5 min. After stimulation, cells were washed three times with cold PBS and then solubilized in 500 µl of PBS-TDS lysis buffer (PBS with 1% Triton X-100, 0.5% Sodium Deoxycholate, 0.1% SDS, 1 mM EDTA, 1 mM PMSF, 2 µg/ml Aprotinin, 5 µg/ml Leupeptin, 1 µg/ml Pepstatin, 2 mM Na₃VO₄). After centrifugation, protein concentration in supernatant was determined by bicinchoninic acid (BCA) protein assay, and 500 µg of lysate was used for immunoprecipitation with antibody against IGF-1Rβ (H-60) followed by western blotting to detect the phosphorylated IGF-1R (pY99) and total IGF-1R.

To detect the phosphorylated Akt and Erk, 50 µg of cell lysate was used for sodium dodecyl sulfate–polyacrylamide gel electrophoresis (SDS–PAGE), and the proteins were then transferred onto nitrocellulose membrane for immunoblotting with phosphorylated Akt antibody (Akt pS473) or phosphorylated Erk antibody (pT202/Y204). The expression level of total Akt and Erk was also blotted and used as a loading control.

2.3. Cell viability assay

We performed *in vitro* cell viability assay using Cell Proliferation Kit II (XTT) (Roche) by following the recommended procedure from manufacturer. Briefly, CNE-2 cells were seeded into 96-well plates (4000 cells/well) and incubated for overnight (37 °C, 5% CO₂). Cells were treated with PPP (0, 0.05, 0.5, 1, and 2.5 µM) for 24 h or 48 h. A 50 µl of XTT reagent was added to each well 4 h before the end of PPP treatment. The spectrophotometrical absorbance of the samples was measured by ELISA reader. Cell viability curve was depicted from the absorbance results. The assay was repeated for three times.

2.4. Fluorescent tubulin micrographs

After overnight culture, CNE-2 cells on coverslips were treated with PBS, PPP (2.5 µM), or vincristine (2.5 µM) for indicated times and then fixed in 4% formaldehyde, permeabilized with 0.5% Triton X-100. Coverslips were blocked with 5% bovine serum albumin for 1 h at room temperature and then incubated with primary mouse anti-α-tubulin antibody (Sigma) for overnight at 4 °C. Coverslips were washed three times with PBS and then incubated with the secondary antibody, i.e., goat-anti-mouse antibody tagged with Texas Red for 1 h. Microtubule staining was determined using a Zeiss immunofluorescence microscope at ×40 magnification.

2.5. Tumor xenograft model

CNE-2 cells with exponential growth were trypsinized and washed with PBS followed by adjusting the cell concentration to 2×10^7 cells/ml with RPMI1640 culture medium. Each nude mouse was subcutaneously injected with 0.2 ml of CNE-2 cells on the right flank. All the mice developed tumor (tumor size >0.5 cm) within 2 weeks of injection. Sixteen tumor-bearing mice (tumor volume between 100–200 mm³) were selected and randomly divided into two groups (i.e., PPP group and DMSO control group) with 8 mice for each group. Each mouse received intraperitoneal injection of either PPP (20 mg/kg; PPP group) or diluted DMSO (same volume as that of PPP; DMSO control group) twice a day for continuous two weeks. Tumor sizes were measured with caliper every 3 days during treatment. Tumor volume (*V*) was calculated by the formula, $V = (L \times S^2)/2$, where *S* and *L* are the shortest and longest diameter of the tumor, respectively. At the end of the experiment, mice were killed and tumors were collected and weighed for calculating tumor growth inhibition using the formula, $[(1 - T/C) \times 100\%]$, where *T* represents the final mean tumor weight in the treatment group and *C* represents the final mean tumor weight in control group.

2.6. Immunohistochemistry staining

Tumor samples, liver tissues, and kidney tissues were collected from mice of each group, fixed in 10% formaldehyde, and embedded in paraffin. The paraffin-embedded tissues were sectioned at 4 µm thicknesses for hematoxylin and eosin (HE) staining.

2.7. Statistical analysis

Statistical analysis was performed by using the Student's *t*-test. A *p* value < 0.05 was considered statistically significant.

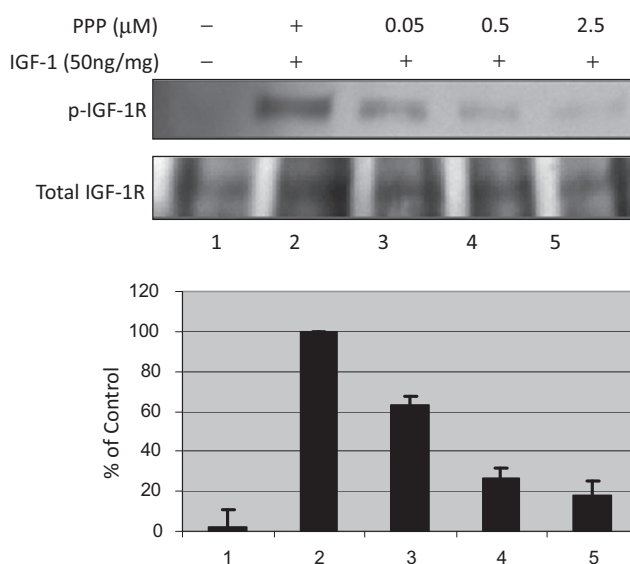


Fig. 1. PPP treatment decreases tyrosine kinase phosphorylation of IGF-1R in CNE-2 cells. Serum starved CNE-2 cells were treated with or without PPP (0, 0.05, 0.5, and 2.5 µM) for 1 h before stimulation with IGF-1 (50 ng/ml) for 5 min. Equal amount of cell lysate from each treatment was used for western blot as indicated. Upper panel, Western blot; lower panel, bar graph shows relative phosphorylation levels of IGF-1R (pY99; p-IGF-1R/total IGF-1R at lane 2 being set as 100%).

3. Results

3.1. PPP treatment suppresses IGF-induced phosphorylation of IGF-1R in CNE-2 cells

As shown in Fig. 1, IGF treatment significantly increased the phosphorylation of IGF-1R in CNE-2 cells (lane 2 vs. lane 1 in Fig. 1), and pretreatment of the cells with PPP for 1 h suppressed the IGF-induced IGF-1R phosphorylation in a dose-dependent manner (lanes 3, 4, and 5 vs. lane 2, respectively in Fig. 1).

3.2. PPP treatment suppresses IGF-induced phosphorylation of Akt and Erk in CNE-2 cells

Akt and Erk are two major downstream targets of IGF-1R and usually activated by IGF treatment. Therefore, we wondered

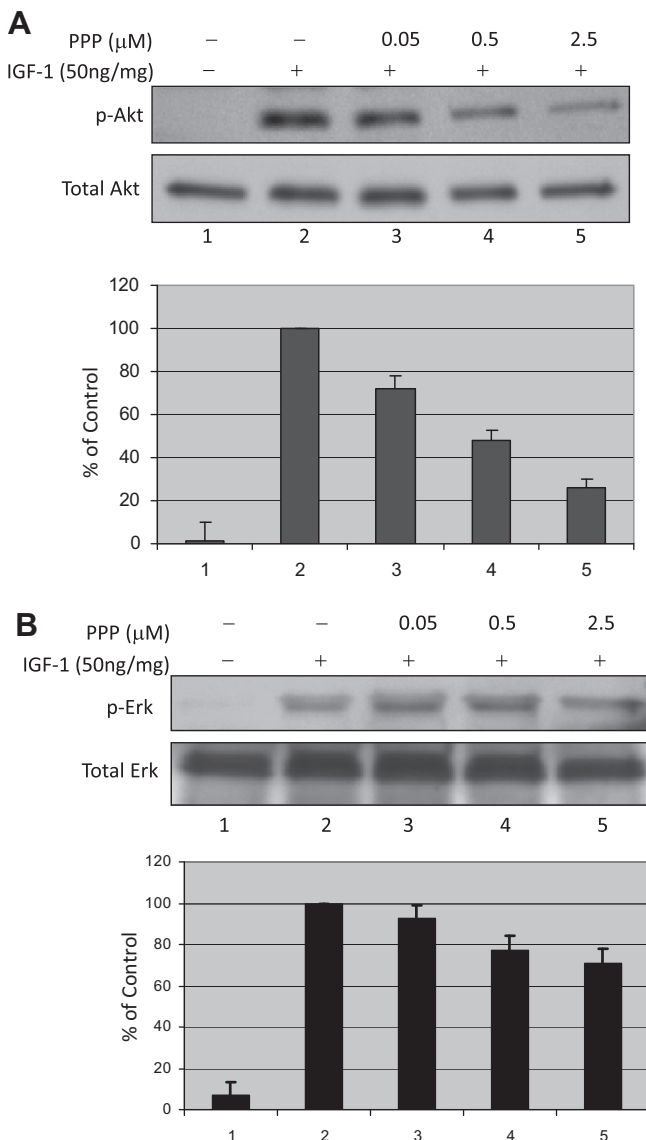


Fig. 2. PPP treatment dose-dependently reduces Akt phosphorylation (Fig. 2A) but marginally decreases Erk phosphorylation (Fig. 2B). CNE-2 cells were treated as the Fig. 1. Equal amount of cell lysate was used for western blot to detect the phosphorylation levels of Akt and Erk. Total Akt and total Erk were blotted to function as loading control. Relative phosphorylation levels (p-Akt/Akt or p-Erk/Erk) were shown in bar graph at the bottom of the corresponding western blot (p-Akt/Akt or p-Erk/Erk at line 2 being set as 100%).

whether PPP could also block the IGF-induced activation of Akt and Erk. As shown in Fig. 2A, PPP pretreatment suppressed the IGF-induced phosphorylation of Akt (p-S472) in a dose-dependent manner (lanes 3, 4, and 5 vs. lane 2 in Fig. 2A, respectively), which is similar to the pattern of IGF-1R observed in Fig. 1, suggesting that PPP inhibits IGF-1R/Akt signaling pathway. In contrast, PPP had little effect on Erk phosphorylation at low dose (i.e., 0.05 μ M) and only showed moderate inhibition at higher doses (i.e., 0.5 μ M and 2.5 μ M) (lanes 3, 4, and 5 vs. lane 2 in Fig. 2B, bar graph).

3.3. PPP inhibits the proliferation of CNE-2 cells

To investigate the effects of PPP on tumor cell proliferation, we treated CNE-2 cells with different doses of PPP for different time points (i.e., 24 h and 48 h) and found that PPP dose-dependently inhibited the proliferation of CNE-2 cells at both time points (Fig. 3). Moreover, 48-h PPP treatment showed suppression in CNE-2 cell proliferation more efficiently than 24-h treatment (Fig. 3). The IC₅₀ for 48-h treatment is ≤ 0.5 μ M, which is much lower than that for 24-h treatment (IC₅₀ ≤ 1.0 μ M).

3.4. PPP slightly inhibits microtubule assembly in CNE-2 cells

To clarify whether the cytotoxic effects of PPP on CNE-2 cells come from its inhibition of microtubule assembly, we treated the CNE-2 cells with PBS, PPP (2.5 μ M), and vincristine (2.5 μ M), a microtubule assembly inhibitor, for 1, 12, and 24 h. We did not incubate cells with PPP for 48 h due to the death of almost 90% cells (Fig. 3). As shown in Fig. S1A, we did not observe any differences about α -tubulin staining among CNE-2 cells treated with PPP and PBS for 1 h, a time point when the marked inhibition of IGF-1R/Akt pathway was observed in PPP-treated cells (Figs. 1 and 2A). The majority of CNE-2 cells treated with PPP for 12 h had clear tubulin staining; however, many cells treated with vincristine for 12 h showed blurry tubulin staining (Fig. S1B). After 24 h treatment, a clear staining of tubulin disappeared in vincristine-treated cells but still appeared in a number of PPP-treated cells (Fig. S1C). It is worth noting that 24-h PPP treatment induced about 65% reduction of cell survival in our experimental condition (Fig. 3). Therefore, we assumed that the cells with blurry tubulin staining might be those dying cells. Taken together, these results suggest that PPP slightly affects microtubule assembly, if there is any, only after long time treatment in CNE-2 cells.

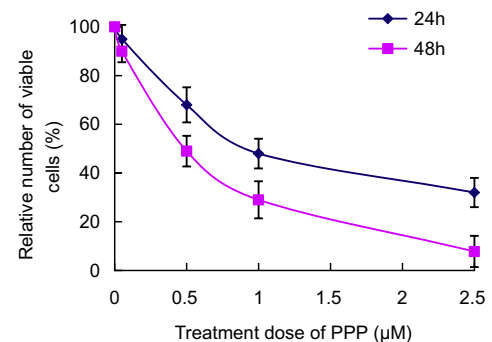


Fig. 3. PPP inhibits CNE-2 cell proliferation *in vitro*. CNE-2 cells were seeded into 96-well plate and cultured at 37 °C, 5% CO₂ overnight. Cells were then treated with PPP (0, 0.05, 0.5, 2.5 μ M) for 24 and 48 h, respectively, followed by XTT assay ($n = 8$). The experiment was repeated for 3 times. Error bar shows \pm SD.

Table 1

Comparison of mouse body weight and tumor volume before PPP treatment.

Group	Mouse body weight (g)	Tumor volume (mm ³)
DMSO	17.18 ± 1.64	102.98 ± 22.69
PPP	17.85 ± 1.23	100.46 ± 23.17
<i>t</i> value	0.932	0.219
<i>p</i> value	0.367	0.830

3.5. PPP suppresses CNE-2 tumor growth *in vivo*

We then investigate the antitumor effects of PPP using NPC mouse model. As shown in Table 1, there were no significant difference in tumor volume before treatment between the control group mice and PPP group mice ($p = 0.83$). However, the tumor grew much slower after PPP treatment (Fig. 4). Consistently, the average tumor volume was much smaller (Table 2) and the average tumor mass was much less (Table 3) in PPP treated group than those in control group, respectively, suggesting that PPP suppressed the CNE-2 tumor growth *in vivo*.

3.6. PPP shows no toxicity in NPC mouse model

To evaluate the toxicity of PPP, we collected liver tissues and kidney tissues of mice from both groups and performed hematoxylin and eosin (H&E) staining. However, we found no obvious morphological and pathological changes in these tissues from both group mice (data not shown).

4. Discussion

IGF-1R plays important roles in carcinogenesis and cancer progression, and targeting IGF-1R as a potential therapeutic strategy has been widely investigated in human cancers [9,18]. However, few of these studies focus on NPC. IGF-1R is highly

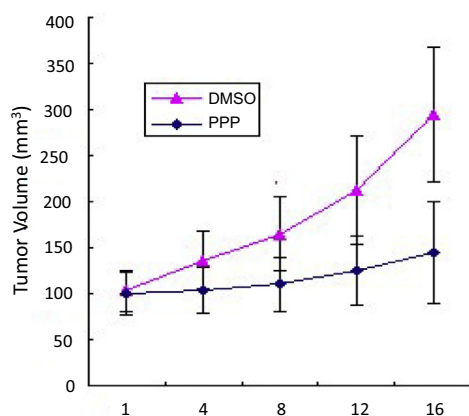


Fig. 4. PPP suppresses CNE-2 tumor growth in nude mice. Tumor-bearing nude mice were intraperitoneally injected with PPP or DMSO, and tumor growth was monitored by measuring tumor volume every 3 days ($n = 8$). Error bar shows \pm SD.

Table 2

Effects of PPP on tumor growth (volume).

PPP treatment	Control group	PPP group	<i>t</i>	<i>p</i>
Day 1	102.98 ± 22.69	100.46 ± 23.17	0.219	0.83
Day 4	136.31 ± 31.13	103.89 ± 24.85	2.302	0.037
Day 8	165.17 ± 40.14	110.26 ± 29.43	3.121	0.008
Day 12	212.37 ± 59.07	124.82 ± 38.05	3.524	0.004
Day 16	294.20 ± 72.94	144.53 ± 55.29	4.625	0.000

Table 3

Comparison of average weight of tumors at the end of PPP treatment.

Group	Average weight of tumors	<i>p</i>
Control	0.22 ± 0.11	0.005
PPP	0.13 ± 0.07	

expressed in both NPC specimens and cell lines, and the expression level of IGF-1R significantly associates with NPC progression [16,19], suggesting that IGF-1R may be a therapeutic target in NPC. Targeting both epidermal growth factor receptor (EGFR) and IGF-1R by siRNAs decreases NPC cell proliferation *in vitro*; however, targeting IGF-1R alone by siRNA has little effect on cancer cell growth [20], suggesting the low efficiency of IGF-1R siRNA in suppressing NPC cell growth. In contrast to siRNA, we demonstrated here that targeting IGF-1R by the small molecular inhibitor, PPP, not only significantly inhibited NPC cell proliferation *in vitro* but also effectively suppressed tumor growth *in vivo*. Our study provides a rationale for clinical use of PPP in NPC therapy. To our knowledge, this is the first study of that PPP shows strong antitumor effect in mice with xenografted NPC.

PPP specifically inhibits the phosphorylation of IGF-1R at Tyr1136, which is crucial for Akt activation, and therefore reduces Akt phosphorylation with little effects on Erk phosphorylation in solid tumors [10,21], but not in myeloma [15]. In our study, treatment of NPC cells with PPP markedly reduced the phosphorylation of both IGF-1R and Akt but marginally suppressed the phosphorylation of Erk, suggesting that the function of PPP in NPC cells predominantly through its down-regulation of IGF-1R/Akt pathway rather than EGF-1R/Erk pathway. Our study is consistent with previous reports in other cancer types including melanoma [21], glioblastoma [12], and osteosarcoma [22].

It is worth noting that PPP was recently reported to inhibit esophageal squamous carcinoma cell (ESCC) growth *in vitro* through an alternative mechanism by inhibiting microtubule assembly rather than IGF-1R/Akt pathway [23]. This alternative mechanism seems to be different from that in our study and others [12,21,24], because we observed no PPP-induced microtubule toxicity in CNE-2 cells after one-hour treatment and slight toxicity after 12-h treatment and moderate toxicity after 24-h treatment. However, the cells with blurry tubulin staining after 24-h treatment were probably those dying cells induced by PPP. The discrepancy may result from the differences of cancer cell types and doses used in these studies. In fact, we used lower doses of PPP (i.e., $\leq 2.5 \mu\text{M}$) in our *in vitro* study; however, Wu et al. used much higher dose of PPP (i.e., $10 \mu\text{M}$) in most of their study in ESCC [23], and, as they indicated, the inhibitory effect of PPP on microtubule assembly was only observed at its relatively higher concentrations [23]. In addition, we detected a dramatic down-regulation of the phosphorylation of both IGF-1R and Akt after one-hour treatment with low dose PPP ($\leq 2.5 \mu\text{M}$) in our study. In contrast, Wu et al. did not observe any changes of IGF-1R/Akt pathway in ESCC cells treated even with much higher dose (i.e., $10 \mu\text{M}$) for longer time (i.e., 24 and 48 h). Finally, we observed about 65% growth inhibition in cells treated with $0.5 \mu\text{M}$ PPP for 24 h; However, less than 30% inhibition, showed as survival index, was detected in most ESCC cell lines treated with $0.5 \mu\text{M}$ PPP for 72 h [23]. These results, taken together, suggest the different cell types may have different sensitivities to PPP, and therefore, different mechanisms could be activated in different cancer cells due to their different cellular contents.

Recent results from targeting IGF-1R phase III clinical trials have shown little clinical benefit in cancer therapy when using anti-IGF-1R antibodies, and some trials have to be abandoned due to unexpected toxicity [18]. Compared to the IGF-1R antibodies, PPP

is a more attractive and safer IGF-1R inhibitor for cancer therapy. PPP has a high specificity for IGF-1R without affecting insulin receptor, a highly homologous of IGF-1R [10], which therefore reduces the unexpected toxicity of PPP. Indeed, PPP has shown little toxicity in rodents [10] and a low possibility to develop drug-resistance *in vitro* after long-term treatment [21]. In addition, PPP is more effective in suppressing melanoma cell growth *in vitro* than other anti-tumor agents, including Imatinib mesylate, cisplatin, 5-FU, and Doxorubicin [24]. These studies, taken together, suggest the efficiency and safety of using PPP in cancer therapy. Consistent to the previous studies, we found that systemically intraperitoneal injection of PPP (20 mg/kg) effectively suppressed tumor growth but showed no obvious toxicity in mice with xenografted NPC, further supporting the potential safety and efficiency of PPP in treatment of human cancer.

Although early stage of NPC is highly sensitive to radiotherapy [25,26], the treatment of advanced NPC with metastasis is still a clinical challenge due to its low response to current therapies and the high toxicity related to combination therapeutics. It is, therefore, an urgent need to develop novel therapeutics for advanced NPC. PPP down-regulates MMPs expression and consequently inhibits tumor cell invasion and migration [11,27], suggesting PPP may inhibit tumor metastasis *in vivo*. Therefore, our future study will investigate whether PPP can suppress NPC metastasis *in vivo* and produce anti-tumor growth effects on metastasized NPC.

Acknowledgments

We thank Professors Olle Larsson and Leonard Girnita from Cancer Center Karolinska, Karolinska Institutet for kindly providing us with PPP and technical support. This study was supported by key program of science fundation from the health department of Hubei Province (Foundation No. WJ301140502).

Appendix A. Supplementary data

Supplementary data associated with this article can be found, in the online version, at <http://dx.doi.org/10.1016/j.bbrc.2013.08.050>.

References

- [1] X. Sun, L.P. Tong, Y.T. Wang, Y.X. Wu, H.S. Sheng, L.J. Lu, W. Wang, Can global variation of nasopharynx cancer be retrieved from the combined analyses of IARC cancer information (CIN) databases?, *Plos One* 6 (2011).
- [2] T. Yoshizaki, M. Ito, S. Muro, N. Wakisaka, S. Kondo, K. Endo, Current understanding and management of nasopharyngeal carcinoma, *Auris. Nasus. Larynx* 39 (2012) 137–144.
- [3] A.T. Chan, Nasopharyngeal carcinoma, *Ann. Oncol.* 21 (Suppl. 7) (2010) vii 308–312.
- [4] A.W. Lee, W.T. Ng, Y.H. Chan, H. Sze, C. Chan, T.H. Lam, The battle against nasopharyngeal cancer, *Radiother. Oncol.* 104 (2012) 272–278.
- [5] E.P. Hui, S.F. Leung, J.S. Au, B. Zee, S. Tung, D. Chua, W.M. Sze, C.K. Law, T.W. Leung, A.T. Chan, Lung metastasis alone in nasopharyngeal carcinoma: a relatively favorable prognostic group. A study by the Hong Kong nasopharyngeal carcinoma study group., *Cancer* 101 (2004) 300–306.
- [6] A. Bennisroune, A. Gardin, D. Aunis, G. Cremel, P. Hubert, Tyrosine kinase receptors as attractive targets of cancer therapy, *Crit. Rev. Oncol. Hematol.* 50 (2004) 23–38.
- [7] M.A. Lemmon, J. Schlessinger, Cell signaling by receptor tyrosine kinases, *Cell* 141 (2010) 1117–1134.
- [8] A.M. Xu, P.H. Huang, Receptor Tyrosine Kinase Coactivation Networks in Cancer, *Cancer Res.* 70 (2010) 3857–3860.
- [9] M. Hewish, I. Chau, D. Cunningham, Insulin-like growth factor 1 receptor targeted therapeutics: novel compounds and novel treatment strategies for cancer medicine, *Recent Pat. Anticancer Drug Discov.* 4 (2009) 54–72.
- [10] A. Girnita, L. Girnita, F. del Prete, A. Bartolazzi, O. Larsson, M. Axelson, Cyclolignans as inhibitors of the insulin-like growth factor-1 receptor and malignant cell growth, *Cancer Res.* 64 (2004) 236–242.
- [11] A. Girnita, C. All-Ericsson, M.A. Economou, K. Astrom, M. Axelson, S. Seregard, O. Larsson, L. Girnita, The insulin-like growth factor-I receptor inhibitor picropodophyllin causes tumor regression and attenuates mechanisms involved in invasion of uveal melanoma cells, *Clin. Cancer Res.* 12 (2006) 1383–1391.
- [12] S. Yin, A. Girnita, T. Stromberg, Z. Khan, S. Andersson, H. Zheng, C. Ericsson, M. Axelson, M. Nister, O. Larsson, T.J. Ekstrom, L. Girnita, Targeting the insulin-like growth factor-1 receptor by picropodophyllin as a treatment option for glioblastoma, *Neuro. Oncol.* 12 (2010) 19–27.
- [13] A. Klinakis, M. Szabolcs, G. Chen, S. Xuan, H. Hibshoosh, A. Efstratiadis, Igf1r as a therapeutic target in a mouse model of basal-like breast cancer, *Proc. Natl. Acad. Sci. USA.* 106 (2009) 2359–2364.
- [14] X. Lu, L. Wang, J. Mei, X. Wang, X. Zhu, Q. Zhang, J. Lv, Picropodophyllin inhibits epithelial ovarian cancer cells in vitro and in vivo, *Biochem. Biophys. Res. Commun.* 435 (2013) 385–390.
- [15] E. Menu, H. Jernberg-Wiklund, T. Stromberg, H. De Raeve, L. Girnita, O. Larsson, M. Axelson, K. Asosingh, K. Nilsson, B. Van Camp, K. Vanderkerken, Inhibiting the IGF-1 receptor tyrosine kinase with the cyclolignan PPP: an in vitro and in vivo study in the 5T33MM mouse model, *Blood* 107 (2006) 655–660.
- [16] S. Yin, X. Zhou, T. Peng, J. Li, X. Jiang, Significance of the expression of insulin-like growth factor-1 receptor in nasopharyngeal carcinoma, *J. Clin. Otorhinolaryngol. Head Neck Surg.* 22 (2008) 874–877.
- [17] C.T. Lin, W.Y. Chan, W. Chen, H.M. Huang, H.C. Wu, M.M. Hsu, S.M. Chuang, C.C. Wang, Characterization of seven newly established nasopharyngeal carcinoma cell lines, *Lab. Invest.* 68 (1993) 716–727.
- [18] M. Pollak, The insulin receptor/insulin-like growth factor receptor family as a therapeutic target in oncology, *Clin. Cancer Res.* 18 (2012) 40–50.
- [19] Y. Yuan, X. Zhou, J. Song, X. Qiu, J. Li, L. Ye, X. Meng, D. Xia, Expression and clinical significance of epidermal growth factor receptor and type 1 insulin-like growth factor receptor in nasopharyngeal carcinoma, *Ann. Otol. Rhinol. Laryngol.* 117 (2008) 192–200.
- [20] Y.L. Yuan, X.H. Zhou, J. Song, X.P. Qiu, J. Li, L.F. Ye, Dual silencing of type 1 insulin-like growth factor and epidermal growth factor receptors to induce apoptosis of nasopharyngeal cancer cells, *J. Laryngol. Otol.* 122 (2008) 952–960.
- [21] D. Vasilcanu, A. Girnita, L. Girnita, R. Vasilcanu, M. Axelson, O. Larsson, The cyclolignan PPP induces activation loop-specific inhibition of tyrosine phosphorylation of the insulin-like growth factor-1 receptor. Link to the phosphatidylinositol-3 kinase/Akt apoptotic pathway, *Oncogene* 23 (2004) 7854–7862.
- [22] Z. Duan, E. Choy, D. Harmon, C. Yang, K. Ryu, J. Schwab, H. Mankin, F.J. Hornicek, Insulin-like growth factor-I receptor tyrosine kinase inhibitor cyclolignan picropodophyllin inhibits proliferation and induces apoptosis in multidrug resistant osteosarcoma cell lines, *Mol. Cancer Ther.* 8 (2009) 2122–2130.
- [23] X. Wu, L. Sooman, M. Wickstrom, M. Fryknas, C. Dyrager, J. Lennartsson, J. Gullbo, Alternative cytotoxic effects of the postulated IGF-1R inhibitor picropodophyllin (PPP) in vitro, *Mol. Cancer Ther.* 12 (2013) 1526–1536.
- [24] M.A. Economou, S. Andersson, D. Vasilcanu, C. All-Ericsson, E. Menu, A. Girnita, L. Girnita, M. Axelson, S. Seregard, O. Larsson, Oral picropodophyllin (PPP) is well tolerated in vivo and inhibits IGF-1R expression and growth of uveal melanoma, *Acta. Ophthalmol.* 86 (2008) 35–41. Thesis 4.
- [25] Y. Bensouda, W. Kaikani, N. Ahbeddou, R. Rahhali, M. Jabri, H. Mrabti, H. Boussen, H. Errihani, Treatment for metastatic nasopharyngeal carcinoma, *Eur. Ann. Otorhinolaryngol. Head Neck Dis.* 128 (2011) 79–85.
- [26] B.B. Ma, A.T. Chan, Systemic treatment strategies and therapeutic monitoring for advanced nasopharyngeal carcinoma, *Expert Rev. Anticancer Ther.* 6 (2006) 383–394.
- [27] X. Feng, E. Aleem, Y. Lin, M. Axelson, O. Larsson, T. Stromberg, Multiple antitumor effects of picropodophyllin in colon carcinoma cell lines: clinical implications, *Int. J. Oncol.* 40 (2012) 1251–1258.